Lactate dehydrogenase from the hyperthermophilic bacterium *Thermotoga maritima*: the crystal structure at 2.1 Å resolution reveals strategies for intrinsic protein stabilization

Günter Auerbach[1]*, Ralf Ostendorp[2†], Lars Prade[1‡], Ingo Korndörfer[1§], Thomas Dams[2], Robert Huber[1] and Rainer Jaenicke[2]

Background: L(+)-Lactate dehydrogenase (LDH) catalyzes the last step in anaerobic glycolysis, the conversion of pyruvate to lactate, with the concomitant oxidation of NADH. Extensive physicochemical and structural investigations of LDHs from both mesophilic and thermophilic organisms have been undertaken in order to study the temperature adaptation of proteins. In this study we aimed to determine the high-resolution structure of LDH from the hyperthermophilic bacterium *Thermotoga maritima* (TmLDH), the most thermostable LDH to be isolated so far. It was hoped that the structure of TmLDH would serve as a model system to reveal strategies of protein stabilization at temperatures near the boiling point of water.

Results: The crystal structure of the extremely thermostable TmLDH has been determined at 2.1 Å resolution as a quaternary complex with the cofactor NADH, the allosteric activator fructose-1,6-bisphosphate, and the substrate analog oxamate. The structure of TmLDH was solved by Patterson search methods using a homology-based model as a search probe. The native tetramer shows perfect 222 symmetry. Structural comparisons with five LDHs from mesophilic and moderately thermophilic organisms and with other ultrastable enzymes from *T. maritima* reveal possible strategies of protein thermostabilization.

Conclusions: Structural analysis of TmLDH and comparison of the enzyme to moderately thermophilic and mesophilic homologs reveals a strong conservation of both the three-dimensional fold and the catalytic mechanism. Going from lower to higher physiological temperatures a variety of structural differences can be observed: an increased number of intrasubunit ion pairs; a decrease of the ratio of hydrophobic to charged surface area, mainly caused by an increased number of arginine and glutamate sidechains on the protein surface; an increased secondary structure content including an additional unique 'thermohelix' (αT) in TmLDH; more tightly bound intersubunit contacts mainly based on hydrophobic interactions; and a decrease in both the number and the total volume of internal cavities. Similar strategies for thermal adaptation can be observed in other enzymes from *T. maritima*.

Addresses: [1]Max-Planck-Institut für Biochemie, Abt. Strukturforschung, 82152 Martinsried, Germany and [2]Universität Regensburg, Institut für Biophysik und Physikalische Biochemie, 93040 Regensburg, Germany.

Present addresses: [†]Purdue University, Department of Biological Sciences, West Lafayette, Indiana 47907, USA, [‡]Novartis Pharma AG, K-681.5.07, 4002 Basel, Switzerland and [§]University of Oregon, Institute of Molecular Biology, Eugene, Oregon 97403, USA.

*Corresponding author.
E-mail: auerbach@biochem.mpg.de

Dedicated to Professor Hugo Fasold on the occasion of his 65th birthday.

Key words: crystal structure, hyperthermophile, lactate dehydrogenase, protein stability, *Thermotoga maritima*

Received: **23 March 1998**
Revisions requested: **14 April 1998**
Revisions received: **29 April 1998**
Accepted: **30 April 1998**

Structure 15 June 1998, **6**:769–781
http://biomednet.com/elecref/0969212600600769

Introduction

As all the early branches of the phylogenetic tree are represented by hyperthermophilic organisms (organisms with physiological temperatures above 80°C), they are considered to be a primordial form of life from which subsequent species descended [1]. Within the bacteria, *Thermotoga maritima* (Tm) grows at temperatures between 55–90°C having an optimum growth temperature of ~80°C. *T. maritima* is, therefore, one of the most thermophilic organotrophs to be isolated so far [2].

Various enzymes from *T. maritima* have been characterized in the past. *In vitro* experiments aimed to unravel differences in the physiological behaviour of these enzymes compared to their less stable counterparts have focused mainly on their physicochemical features and their folding pathways. The enzymes that have been investigated are dihydrofolate reductase (TmDHFR) [3], enolase [4], ferredoxin (TmFd) [5], glutamate dehydrogenase (TmGluDH) [6], glyceraldehyde-3-phosphate dehydrogenase (TmGAPDH) [7–10], lactate dehydrogenase (TmLDH) [11–15], phosphoglycerate kinase (TmPGK) [16,17], phosphoribosyl anthranilate isomerase (TmPRAI) [18], triosephosphate isomerase (TmTIM) [16], and xylanase [19]. All of these enzymes show anomalously high intrinsic stabilities, with denaturation temperatures above

Table 1

Characteristics of LDH from organisms with different physiological temperatures*.

	TmLDH	BsLDH	BlLDH	LcLDH	SsLDH		SaLDH	
Phylogenetic domain	Bacteria	Bacteria	Bacteria	Bacteria	Eukarya		Eukarya	
Physiological temp (°C)† (range/optimum)	50–90/80	40–65/52	37–41/39	30–40/35	37/37		20/20	
Number of amino acids	319	317	320	325	331		329	
Sequence identity (%)‡	–	39.5	40.3	41.2	40.5		36.8	
Sequence similarity (%)‡	–	60.0	60.9	60.4	51.5		52.1	
Thermal denaturation (°C)§	91	60	nd¶	nd¶	45		nd¶	
PDB code	1a5z**	1ldn**	1lld**	1llc**	9ldt**	9ldb	1ldm**	6ldh
Resolution (Å)	2.1	2.5	2.0	3.0	2.0	2.2	2.1	2.0
Rmsd vs TmLDH (Å)#	–	2.15	1.57	2.36	2.21	2.18	1.78	1.99
Complexed ligands¥	NADH, Oxm, FBP	NADH, Oxm, FBP	NADH	FBP	NADH, Oxm	NADH	NADH, Oxm	(apoenzyme)

*Tm, *Thermotoga maritima*; Bs, *Bacillus stearothermophilus*; Bl, *Bifidobacterium longum*; Lc, *Lactobacillus casei*; Ss, *Sus scrofa* (pig); Sc, *Squalus acanthias* (dogfish). †Physiological temperature of source organism. ‡Amino acid sequence identity and similarity versus TmLDH. §Taken from [52]. #Rmsd, root mean square deviation. ¥Oxm, oxamate; FBP, fructose-1,6-bisphosphate. ¶nd, not determined. **Used for structural comparison. For references see text.

the optimum growth temperature of the bacterium. Recently, the three-dimensional crystal structures of several of these enzymes have been determined: TmFd [20], TmGAPDH [21], TmGluDH [22], TmPGK [23,24], TmPRAI [25], and TmTIM (D Maes and RK Wierenga, personal communication). As a result of these studies, these ultrastable enzymes have been shown to be highly homologous to their mesophilic counterparts with respect to amino acid sequence, overall fold and catalytic mechanism.

LDH is one of the best characterized enzymes in terms of protein evolution, folding, catalytic mechanism, stability, and three-dimensional structure [26,27]. The enzyme catalyzes the interconversion of the oxoacid, pyruvate, and the hydroxy acid, lactate, using the NADH/NAD^+ pair as a redox cofactor [28]. The reaction mechanism of LDH has been analyzed by classical steady-state methods and transient kinetics [29]. As a large number of gene and amino acid sequences of LDHs from psychrophilic, mesophilic, and thermophilic organisms are known, LDH has become a paradigm for studying the structural basis for temperature adaptation at the protein and DNA level [30].

Sequence comparisons of thermophilic, mesophilic, and psychrophilic LDHs suggested that a number of temperature-related amino acid substitutions correlated with their respective intrinsic stabilities [31–37]. Despite observed tendencies within homologous enzymes, no general and unequivocal rules for the thermal stabilization of proteins have been obtained. Statistical analyses, however, indicate that marginal alterations of intra- and intermolecular interactions allow the flexibility of proteins to be adjusted so that full catalytic function is maintained at varying temperatures [38,39].

Until recently, the approach to learn more about the phenomenon of extreme intrinsic protein stability by comparison of homologous protein species from thermophilic and mesophilic organisms was limited mainly to physicochemical studies. High-resolution three-dimensional structures of proteins from various temperature ranges were not available [39–41]. LDH is an exception for which both detailed physicochemical and structural information from mesophilic, thermophilic and hyperthermophilic variants have been accumulated. High-resolution crystal structures of LDH have been determined for the enzyme from *Bacillus stearothermophilus* (BsLDH) [42,43], *Lactobacillus casei* (LcLDH) [44], *Bifidobacterium longum* (BlLDH) [45], *Squalus acanthias* (dogfish; SaLDH) [46–48], mouse [49], *Sus scrofa* (pig; SsLDH) [50], and *Plasmodium falciparum* (PfLDH) [51]. As the most thermostable LDH isolated so far, TmLDH extends the series of known LDH structures from mesophilic, via moderately thermophilic to a hyperthermophilic species (Table 1). This new structure allows the comparison of the three-dimensional structures of the enzyme in the light of a detailed physical and enzymatic characterization [12–15,52].

The gene encoding TmLDH has been cloned and functionally expressed in *Escherichia coli* [13]. The enzyme has been extensively characterized and crystallized [14]. Its extreme intrinsic stability is reflected by both long-term

stability at temperatures up to 85°C and catalytic activity above 100°C. As a unique feature of this enzyme, the recombinant protein monomer assembles into both homotetrameric and homooctameric molecules with identical spectral properties [15]. Both species have enzymatic activity and exhibit highly cooperative dissociation transitions at guanidinium chloride concentrations up to 2.0 M at 25°C.

Structural comparisons of homologous proteins from thermophilic and mesophilic organisms have revealed several strategies to enhance protein stability. In the more thermostable molecules, improved hydrophobic [53,54] and electrostatic [55,56] interactions as well as hydrogen bonding [57,58] are responsible for a more rigid and, therefore, more stable protein. Furthermore, improved intersubunit contacts within oligomeric proteins [59,60] and the reduction of the number and volume of cavities [61] play a role in protein stabilization. Other mechanisms discussed in this context are: a tendency to form high order oligomers [3], an increase in secondary structure accompanied by a decrease in the length of surface loops [23], and improved stabilization of α helices by the introduction of helix-forming residues or helix capping [62–66]. Available data clearly indicate that the intrinsic thermal stability of proteins cannot be explained by a single mechanism [39].

The aims of this work were to elucidate further the structural determinants of the thermal stability of TmLDH and to search for generally applicable strategies of protein stabilization in this hyperthermophilic organism. Here we report the crystal structure determination, the refinement and the analysis of tetrameric TmLDH at 2.1 Å resolution. The structure was determined by Patterson search methods using a homology-based model [14] as a search probe. The refined model was compared with the crystal structures of BsLDH, BlLDH, LcLDH, SsLDH, and SaLDH (Table 1).

Results

The monomer

Structural alignment of the TmLDH monomer with other LDH structures (Table 1) shows a high degree of conservation of the overall three-dimensional fold [26]. The protein consists of two major domains: the nucleotide-binding domain, comprising a twisted N-terminal six-stranded β sheet; and the catalytic domain located within the C-terminal half of the polypeptide chain. The final model of TmLDH comprises the amino acid residues Met22–Asn333; the model lacks seven residues at the C terminus which were not clearly defined in the electron-density map and probably adopt an α-helical conformation.

The tetramer

As there is one monomer in the asymmetric unit of the tetragonal space group, the native tetramer of TmLDH is built up by crystallographic twofold axes yielding precise 222 symmetry (Figure 1). Subunit contacts can occur along the mutually perpendicular molecular axes P, Q, and R [26]. Q axis related subunit contacts involve residues belonging to helices αB, αC, α2F, α2G, and α3G; contacts between P axis related subunits involve residues from the secondary structure elements α2F, βG, βH, α3G, βL, and βM.

The active site

Structural alignment of the catalytic residues with other LDH structures reveal the active site to be strictly conserved. Presumably, His195 acts as the proton donor/acceptor and Arg109 interacts with the transition-state structure in the reaction. Asp168, next to the catalytic histidine residue, stabilizes the protonated carbonyl binding form of His195. As the active site is not completely closed by the active site surface loop (asl) and a Cd^{2+} ion is bound to the His195 and Asp168 sidechains, Arg109 does not directly anchor the substrate analog oxamate in this structure. The distance between Arg85 NH2 and the substrate C1 carbonyl is 8 Å. Because His68 from the neighboring subunit also binds to the Cd^{2+} ion in the active site, Arg148 is not able to anchor the substrate carboxylate group as in other LDH complex structures reported previously [28,67]. Despite these characteristics of the present model, no evidence is found for an altered catalytic mechanism.

Figure 1

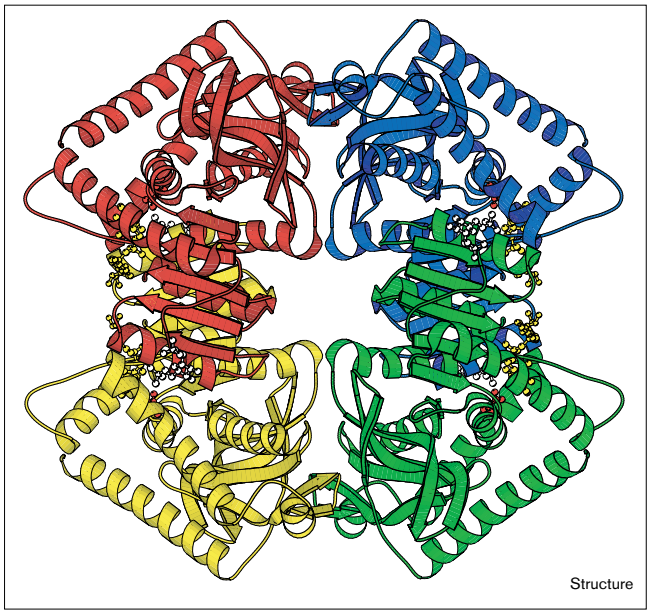

The TmLDH tetramer. Ribbon diagram of the TmLDH tetramer with bound substrate oxamate, cofactor NADH, and the allosteric activator fructose-1,6-bisphosphate (FBP). The subunits are color-coded according to [26]: A, red; B, blue; C, green; D, yellow. The bound ligands are shown in ball-and-stick representation (oxamate, red; NADH, yellow; FBP, white).

Figure 2

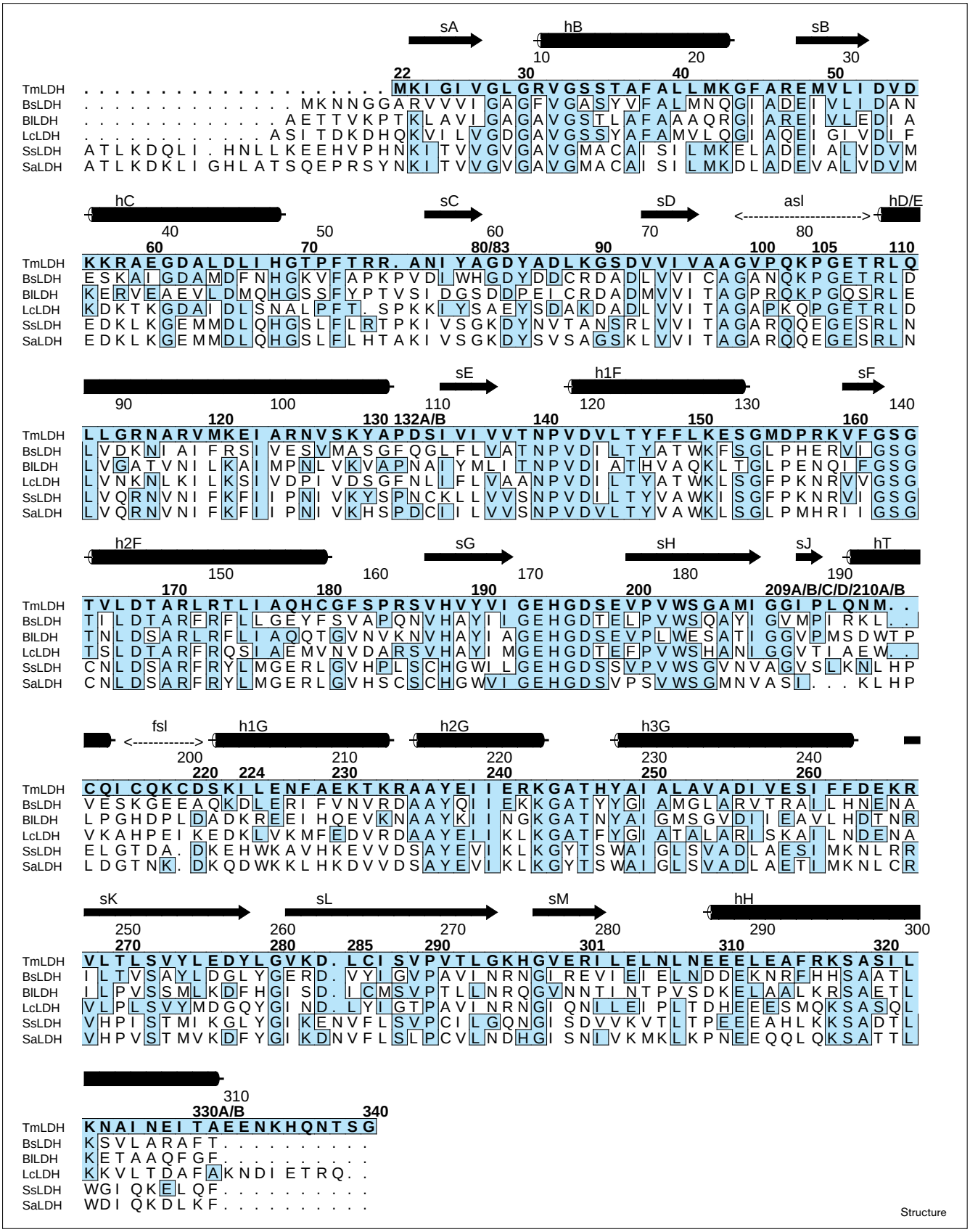
sA
hB
sB
hC
sC
sD
asl
hD/E
sE
h1F
sF
h2F
sG
sH
sJ
hT
fsl
h1G
h2G
h3G
sK
sL
sM
hH
TmLDH
BsLDH
BlLDH
LcLDH
SsLDH
SaLDH
Structure

Figure 2 continued

Structure-based sequence alignment of LDHs. The amino acid sequences of LDH from six organisms were aligned: *T. maritima* (TmLDH), *B. stearothermophilus* (BsLDH), *B. longum* (BlLDH), *L. casei* (LcLDH), pig (SsLDH), and dogfish (SaLDH). Conserved amino acids are marked with blue shaded boxes. The sequence numbering refers to TmLDH in the upper line and to the established LDH numbering system [124] in the lower line (bold face). The secondary structure elements of TmLDH are marked above the sequence: helices are shown as cylinders and β strands as arrows.

Cysteine and arginine residues

Non-essential cysteine residues are often absent in enzymes isolated from hyperthermophiles. With five cysteine residues per monomer, however, TmLDH comprises the highest cysteine content compared to the other LDHs studied [68]. Four of these residues (Cys180, Cys213, Cys216, and Cys219) cluster within a sphere of 6 Å. As the structure reveals neither disulfide linkages nor metal binding at this site, the role of the cysteine cluster remains to be explained.

TmLDH contains a mean of 6.8 ± 0.8 mol% arginine, a value comparable with other thermophilic LDHs; mesophilic LDHs contain a mean arginine content of 3.3 ± 1.5 mol% [68]. Examination of the 18 arginine residues of the TmLDH monomer reveals that they are regularly distributed over the whole molecule and exposed to solvent either at the molecule surface or within the central cavity of the tetramer. Seven arginine residues (Arg47, Arg58, Arg115, Arg125, Arg234, Arg242 and Arg267) are involved in ion pairs either with glutamate or aspartate sidechains and four of them (Arg31, Arg58, Arg74 and Arg301) form hydrogen bonds to mainchain carbonyl groups. Only three arginines (Arg109, Arg171 and Arg173) are completely conserved within the analyzed LDHs (Figure 2).

Ion pairs and hydrogen bonds

A comparison of the six LDH crystal structures reveals that an increased number of intrasubunit ion pairs correlates with a higher growth temperature of the organism (Table 2). The number of intermolecular ion pairs is slightly increased within the prokaryotic LDHs. Except for an increased number of mainchain hydrogen bonds within the TmLDH tetramer, the number of hydrogen bonds in the monomer and tetramer does not differ significantly (data not shown).

Secondary structure elements: additional α helix T

As proposed from spectroscopic measurements, homology modeling, and secondary structure predictions [14], the secondary structure content of TmLDH is increased relative to that observed in other LDHs. Approximately 46% of the residues are found in an α-helical conformation and 23% in β-strand conformation. The difference with other LDHs is significant, as the α helix content of BsLDH, BlLDH, and SsLDH is 42%, and that of SaLDH only 40%. The same tendency is found for β strands: BlLDH contains 22% of its residues in a β-strand conformation, SsLDH 20%, and BlLDH and ScLDH 19% (Table 3).

A significant structural feature contributing to the increased α-helical content of TmLDH is the presence of an additional helix between strand βJ and helix αh1G. This helix shortens the flexible surface loop (fsl) observed in other LDHs by five residues (Figure 3). Although parts of the fsl in the thermophilic BsLDH adopt a nearly helical conformation, this α helix is found only in TmLDH and should be assigned as an additional α helix (αT) comprising amino acid residues Gln210B–Gln214. Recently, 'thermohelices' were also found in cytochrome c_{552} from *Thermus thermophilus* where they function as stabilizing clamps at the surface of the protein [69].

Whereas the α-helix content in TmLDH is increased compared to other LDHs, the strategies for helix stabilization seem to be unaltered. Analyzing the charged residues lining the dipoles of α helices, neither the content of aspartate or glutamate residues around the N termini, nor the content of lysine or arginine residues around the C termini of the helices is significantly different.

Accessible surface area and total volume

The total accessible surface area (ASA) of the six analyzed LDH structures is similar. The amount of hydrophobic surface area of TmLDH is, however, decreased with a concomitant increase in charged surface area: the ratio of hydrophobic to charged surface area in TmLDH is 0.57, BsLDH 0.66, BlLDH 0.76, LcLDH 0.73, SsLDH 0.89,

Table 2

Comparison of intrasubunit ion pairs in LDHs within a distance of 4 Å*.

Ion pairs	TmLDH	BsLDH	BlLDH	LcLDH	SsLDH	ScLDH
Per monomer	17 (32)	16.5 (28.7)	8 (22.5)	8 (20)	10.5 (20)	13 (25)
Per residue	0.05 (0.10)	0.05 (0.09)	0.03 (0.07)	0.03 (0.06)	0.03 (0.06)	0.04 (0.07)

*Values in parentheses represent intrasubunit ion pairs within a distance of 6 Å. Organism names are as defined in Table 1.

Table 3

Secondary structure content of LDH*.

	TmLDH	BsLDH	BlLDH	SsLDH	SaLDH
α Helix	46 (144)	42 (134)	42 (133)	42 (139)	40 (131)
β Strand	23 (72)	22 (71)	19 (58)	20 (67)	19 (63)

*The values given are for the percentage of each type of secondary structure element; values in parentheses refer to the actual number of residues. Organism names are as defined in Table 1.

and SaLDH 0.86. This tendency is found for the monomer as well as for the tetramer (Table 4). In particular, the arginine and glutamate content of the surface area is increased in TmLDH [70]. No clear correlation can be found between thermal stabilization and the total volume of the monomer and tetramer, or to the surface to volume ratio (data not shown).

Subunit interfaces

The free energy term favoring protein association is derived from the decrease in water accessible surface area which occurs upon association of the subunits to form the native quaternary structure. Analyzing the residues in subunit interfaces within a distance of 4 Å, there are 88 Q axis related intersubunit contacts (22 of which are hydrophobic) in TmLDH, 78 (16 hydrophobic) in BsLDH, 63 (nine hydrophobic) in BlLDH, and 66 (eight hydrophobic) in LcLDH. These values indicate that subunits in the thermostable enzymes are more tightly bound. As has been proposed from sequence alignments [52], increased hydrophobicity in the protein core is mainly achieved by the local accumulation of phenylalanine residues lining the central cavity of the tetramer, whereby each subunit provides three phenylalanine residues (Phe24, Phe242, and Phe243). The accessible surface area buried in tetramer contacts of TmLDH is 11,800 Å, which is in the same range as that observed for other LDHs. As mentioned previously, there is no significant increase in the number of ion pairs in intersubunit contacts.

Packing and cavities

Close packing with the concomitant exclusion of bulk solvent has been assumed to be essential in the stabilization of the native state of proteins [71,72]. Despite the preference towards optimal association of amino acids in proteins, packing defects and cavities are observed [73,74].

A criterion for the packing of a protein is given by the fraction of atoms in a protein with zero accessibility [75]. The percentage of buried atoms in the TmLDH and BsLDH monomers is only slightly increased compared to mesophilic LDHs, revealing no clear correlation with thermostability.

The first computational study of internal cavities in proteins was reported by Lee and Richards [76]. We have estimated cavity volumes and surface areas by rolling a sphere of radius 1.4 Å over the surface of the molecule [77]; the results are listed in Table 5. TmLDH has fewer and smaller cavities than its less thermostable counterparts.

Figure 3

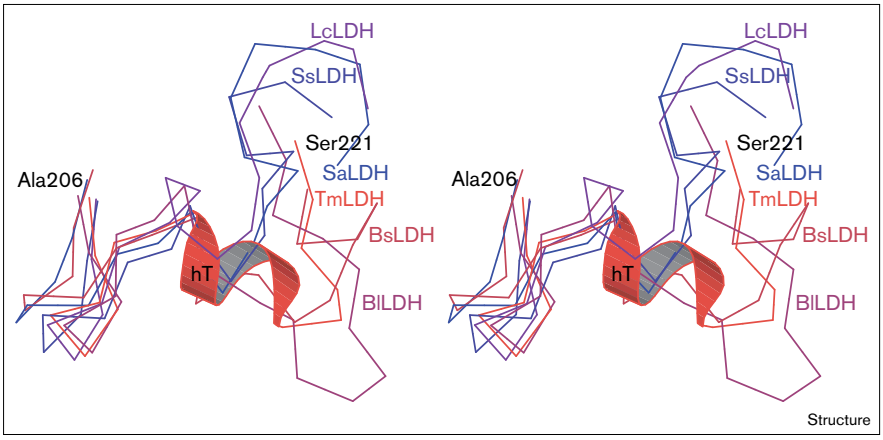

Flexible surface loops of LDHs. Cα trace stereo diagram of the superposition of the flexible surface loop regions of different LDHs: TmLDH amino acid residues 206–221 (red); BsLDH 204–223 (pink); BlLDH 191–212 (magenta); LcLDH 206–221 (purple); SsLDH 206–222 (dark blue); SaLDH 204–221 (light blue).

Table 4

Comparison of accessible surface areas of LDH monomers and tetramers*.

	TmLDH	BsLDH	BlLDH	LcLDH	SsLDH	SaLDH
Monomer						
Total ASA	100 (14,673)	100 (13,714)	100 (14,286)	100 (15,519)	100 (16,050)	100 (16,743)
Hydrophobic	26 (3873)	27 (3734)	29 (4160)	29 (4604)	33 (5438)	32 (5424)
Polar	27 (4011)	31 (4299)	32 (4688)	29 (4569)	28 (4551)	29 (5022)
Charged	46 (6852)	41 (5680)	38 (5438)	40 (6345)	37 (6060)	37 (6296)
Ratio hydrophobic/charged	0.57	0.66	0.76	0.73	0.89	0.86
Tetramer						
Total ASA	100 (46,891)	100 (39,683)	100 (45,435)	100 (45,665)	100 (42,189)	100 (44,730)
Hydrophobic	22 (10,566)	22 (8943)	24 (11,227)	24 (11,340)	26 (11,044)	24 (11,072)
Polar	27 (13,086)	31 (12,445)	31 (14,158)	27 (12,669)	29 (12,385)	29 (13,332)
Charged	50 (23,485)	46 (18,294)	44 (20,048)	47 (21,654)	44 (18,759)	45 (20,325)
Ratio hydrophobic/charged	0.44	0.48	0.55	0.51	0.59	0.53

*The values for the accessible surface area (ASA) are given as percentages; the values in parentheses are the ASA in Å^2. The results were calculated with the program X-PLOR using a probe radius of 1.4 Å. Organism names are as defined in Table 1.

Surface potential

Comparison of the surface potential of the various LDHs reveals a rather positively charged interior of the core region of the TmLDH tetramer (Figure 4). This charge is provided by the arginine residues Arg53, Arg54, Arg135, and Arg279 and the lysine residues Lys246 and Lys274.

Dimerization of the tetramer

Recombinant TmLDH associates into the regular homotetrameric state and also forms homooctameric oligomers [14]. Electron microscopy studies of the two isolated species revealed a globular conformation of the tetrameric form and a dumbbell-shaped form of the octamer [15]. The octamer is, therefore, probably associated as a dimer of tetramers, driven by hydrophobic interactions which we tentatively ascribe to the formation of a four-helix bundle along helices α2G and αH in subunits B and D.

Table 5

Cavities found in LDH monomers*.

	TmLDH	BsLDH	BlLDH
Number of cavities found	2	4	4
Volumes of single cavities (Å^3)	19.8	41.2	59.2
	19.9	29.7	42.7
	–	20.3	41.5
	–	18.5	20.5
Total cavity volume (Å^3)	39.8	109.6	163.5
Total monomer volume (%)	0.08	0.27	0.39

*Values were calculated using a probe radius of 1.4 Å. Organism names are as defined in Table 1.

Homology model of TmLDH

At an earlier stage of our conformational analysis, the crystal structures of BsLDH [43], BlLDH [45], and SaLDH [48] were used to model the three-dimensional structure of TmLDH [14,78]. Comparing the predicted structure with the present crystal structure, a root mean square (rms) difference of 1.38 Å (for 278 aligned Cα atom positions) was calculated. Deviations occur mainly in loop regions, in particular in the active site and in surface loop regions. From the additional secondary structure element αT, it is obvious that homology modeling cannot predict structural features, which are not present in the parent structures. In contrast to the X-ray structure, the model suggested an increase in packing density of the protein core region, leading to a reduced total protein volume. Nevertheless, the homology model did correctly propose a molecule stabilized by an increased number of subunit interactions and intramolecular salt bridges as well as an increase in α-helical content.

Discussion

Amino acid substitutions

Temperature-related amino acid substitutions in LDHs have been classified in order from typical thermostabilizing residues in thermophilic LDHs to thermolabilizing residues in mesophilic LDHs [31,32,34]. Zuber [33] showed that in the case of the moderately thermophilic BsLDH the arginine and glutamate content is increased whereas the lysine content is decreased. Analysis of the amino acid composition of all known prokaryotic LDHs produced no conclusive results, however [68]. In TmLDH, at least, there is a remarkably high proportion of cysteine and arginine residues. Bearing in mind the sensitivity of cysteine residues toward oxidation, this is surprising especially as there is no obvious function for the cysteine cluster.

Figure 4

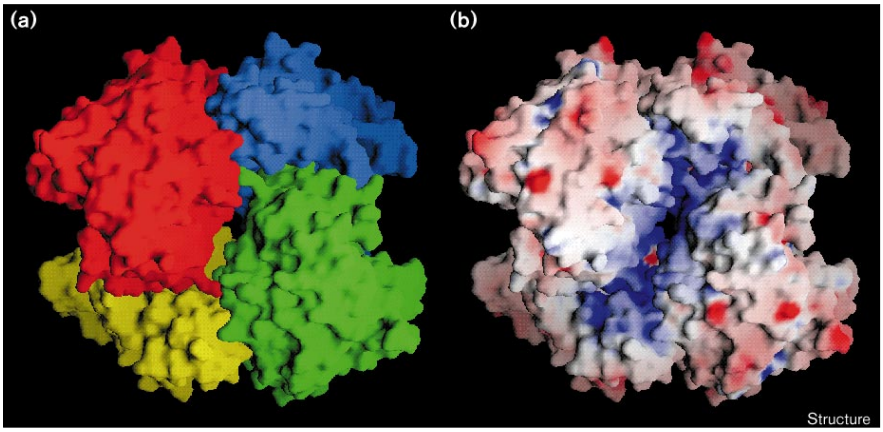

Surface representation of the TmLDH tetramer. **(a)** The TmLDH tetramer colored by subunit: A, red; B, blue; C, green; D, yellow. **(b)** The tetramer in the same orientation as (a) but colored by surface potential (blue, positive; red, negative).

Arginine residues seem to play a role in the stabilization of certain proteins either by forming salt bridges, usually with aspartate or glutamate sidechains, or by forming multiple hydrogen bonds to backbone carbonyl oxygens [79–81]. In TmLDH, mainly nonconserved arginines form ion pairs and/or mainchain hydrogen bonds. Thus, the attribution of additional protein stabilization to an increased number of arginine residues seems to be justified. As the guanidinium group of arginine is the most polar of all the common amino acid sidechains found in proteins, it is not surprising that all arginines in TmLDH are solvent-exposed. Contributions to the intrinsic stability of thermophilic enzymes have also been attributed to additional proline and glycine residues in loop regions, where the stabilizing effect is thought to be due to the entropic destabilization of the denatured state [82]. As all the proline and glycine residues found in TmLDH loop regions also occur in the mesophilic counterparts, they presumably do not play a significant role in the thermophilic stabilization of the native state (Figure 2). Ala→Pro mutations, however, in a thermolysin-like protease have been shown to have a stabilizing effect [83].

Ion pairs

The role of stabilizing electrostatic interactions in proteins is a controversial issue [84,85]. In some cases specific interactions, with charged groups participating in salt bridges, seem to be involved in protein stabilization. The strength of a salt bridge and its contribution to the stability of the folded conformation was estimated to be 3–5 kcal mol^{-1} [86]. At room temperature, surface ion pairs should destabilize the native protein, because of the incomplete coulombic compensation of solvation effects [87]. At high temperatures, however, hydration effects play a less important role resulting in a net stabilizing effect of ion pairs.

Ion pairs [21,23,55,88,89] and ion-pair networks [22,90,91] have been proposed to play a key role in the maintenance of enzyme stability at high temperatures. As shown by site-directed mutagenesis experiments on barnase [92] and TmGAPDH [10,93], clusters of salt bridges seem to be of general importance for both thermodynamic and kinetic stability. The number of intrasubunit ion pairs in TmLDH is increased significantly compared to its mesophilic counterparts, confirming the proposed stabilizing effect of salt bridges.

Secondary structure

In TmLDH, 46% of the amino acid residues are located in α helices and 23% in β strands, both values being remarkably higher than in mesophilic LDHs. Increased hydrogen bonding within secondary structure elements correlates with an increase in rigidity in the protein interior. In the TmLDH tetramer the number of mainchain hydrogen bonds is slightly increased. As indicated by its different conformation in all analyzed crystal structures, one of the most flexible regions of LDH is the fsl. By decreasing its flexibility in TmLDH, the N-terminal part of this loop adopts a helical conformation building a new secondary structure element (helix αT) (Figure 3).

It is known that α helices can be stabilized by charge compensation of their net dipole moment [94], for example by a carboxylate group (aspartate or glutamate) adjacent to their N terminus and an amino group (arginine or lysine) at their C terminus [95]. Mutational experiments on barnase have generated a rank order of amino acid preferences at the C- and N-caps of α helices [96]. As none of these amino acid preferences is found with regard to the α helices in TmLDH, helix capping evidently does not contribute significantly to the thermal stability of TmLDH.

Accessible surface area

Protein–water interactions are of fundamental importance for the folding, as well as the three-dimensional structure and the enzymatic activity of a given protein

Table 6

Comparison of ultrastable enzymes from *Thermotoga maritima*.

	TmLDH	TmGAPDH	TmGluDH	TmPGK	TmFd
Resolution of X-ray structure (Å)	2.1	2.5	3.0	2.0	1.75
Structure comparisons performed with homologous enzymes from	Bs, Bl, Lc, pig, dogfish	Bs, lobster	Pf, Cs	Bs, yeast, pig	Tl, Pf, Dg, Bt, Da
Increased number of intrasubunit ion pairs	+	+	+	+	(No ion pairs)
Decrease of electrostatic and increase of hydrophobic intersubunit contacts	+	+	+	(Monomeric)	(Monomeric)
Increased number of hydrogen bonds	–	+	nd	–	+
Increase of the fraction of buried hydrophobic atoms	+	+	+	nd	nd
Increased secondary structure content	+	nd	–	+	+
Total cavity volume decreased	+	nd	+	nd	(No cavities)
Tendency to form high-order oligomers	+	+	(Not known)	+	(Not known)
Fixing N and C terminus	–	–	–	+	+
Total volume decreased	–	–	–	+	nd
Reference	–	[21]	[22]	[23,24]	[20]

The correlation of each of the listed factors with thermostability is noted: +, correlation with thermostability; –, no correlation; nd, not determined. The enzymes used in the comparison were: LDH, lactate dehydrogenase; GAPDH, glyceraldehyde-3-phosphate dehydrogenase; GluDH, glutamate dehydrogenase; PGK, phosphoglycerate kinase; and Fd, ferredoxin. The organisms from which the enzymes were obtained were: Bl, *Bifidobacterium longum*; Bs, *Bacillus stearothermophilus*; Bt, *Bacillus thermoproteolyticus*; Cs, *Clostridium symbiosum*; Da, *Desulfovibrio africanus*; Dg, *Desulfovibrio gigas*; Lc, *Lactobacillus casei*; Pf, *Pyrococcus furiosus*; and Tl, *Thermococcus litoralis*.

[71,97]. The ASA allows quantification of the extent to which atoms on the protein surface can form contacts with water [76,98]. The term has energetic significance in that it is directly related to hydrophobic free energies: each square Ångström of ASA removed from contact with water yields a gain in free energy of 25 cal mol^{-1} [99]. The reduction of the solvent-accessible surface area and an increase in the fraction of buried hydrophobic atoms have been discussed as stabilizing principles for thermostable proteins in several studies [75]. The decrease in the ratio of hydrophobic to charged surface area in TmLDH suggests that the minimization of the hydrophobic surface area represents an important stabilizing principle in thermophilic LDHs.

Compactness

Cavities are energetically unfavorable due to a loss of van der Waals contacts [100]. The most destabilizing replacements tend to occur in the most rigid parts of a protein structure [101]. Recent work has demonstrated that 'filling' and 'creating' cavities by site-directed mutagenesis can increase or reduce the thermostability of proteins [53,61,102]. The TmLDH monomer has fewer and smaller cavities than the other analyzed LDH structures; a similar result has been reported for TmGluDH [22]. The analysis of subunit interfaces in TmLDH reveals tight dimer contacts due to increased hydrophobic interactions. The number of intersubunit ion pairs is only slightly increased. As the total volumes and surface areas of the monomers or tetramers of the different LDHs are similar, the surface to volume ratio does not correlate with thermal stability.

Oligomerization

Protein stability is accomplished at various levels of the protein structure hierarchy [52]. As various enzymes from thermophilic and hyperthermophilic enzymes are known which exhibit anomalously high states of association, thermal adaptation of proteins seems to be attributable to higher states of subunit assembly. A tendency to form high-order oligomers is found *in vitro* for TmDHFR [3], TmLDH [15], TmGAPDH (G Pappenberger, personal communication), Tm enolase [4], TmTIM, and TmPGK [16,103–105].

Strategies of protein thermostabilization within *T. maritima*

In an attempt to generalize the results derived from the crystal structure of TmLDH, different ultrastable enzymes from the same organism, *T. maritima*, have been compared with regard to possible strategies of thermal adaptation (Table 6). Despite the largely different size and native oligomeric state, an increased number of intrasubunit ion pairs and increased hydrophobic intersubunit interactions indicate similar strategies within the same organism.

Biological implications

Extremely stable enzymes from hyperthermophilic organisms are of considerable interest, as they can be used to improve the efficiency of industrial processes and provide insight into general mechanisms of protein folding and stability. The bacterium *Thermotoga maritima* represents one of the deepest branches within the universal phylogenetic tree and grows at an optimum temperature of around 80 C. *Thermotoga* seems to occupy an intermediate phylogenetic position between the remaining bacteria and the archaea.

Lactate dehydrogenase (LDH) catalyzes the last step in anaerobic glycolysis and can be regarded as one of the most well-characterized enzymes. A comparison of the crystal structure of LDH from *T. maritima* (TmLDH) with five LDH structures from moderately thermophilic and mesophilic organisms reveals a variety of different tendencies, which might contribute collectively to withstand the dissipative action of thermal motion: an increased number of salt bridges within subunits; an additional unique α helix located in a flexible surface loop region of mesophilic species, and an overall increased secondary structure content; a decrease of the ratio of hydrophobic to charged surface area; an increase in hydrophobic subunit interactions; and both a reduced number and total volume of cavities. As many of these stabilizing interactions are cooperative, they cannot be reduced to a sum of pairwise interactions. Treating the results with the necessary caution, the large number of fine structural differences detectable in TmLDH strongly suggest that at least some of them are involved in increasing the thermal stability of this enzyme.

Materials and methods

Protein preparation and crystallization

TmLDH was expressed in *E. coli* at 26°C and purified as described previously [14]. Crystallization experiments were performed at 4°C employing the vapour diffusion technique. Crystals from TmLDH protein (5.0 mg ml^{-1} protein concentration), buffered in 0.1 M HEPES buffer pH 7.5, appeared in the presence of 1.0 M sodium acetate, 250 mM oxamate, 150 mM NADH, 150 mM fructose-1,6-bisphosphate, and 50 mM cadmium sulfate and grew within a few days to a size of 150 μm × 270 μm [14]. The crystals belong to the space group $I4_122$ with lattice constants a = b = 106.33 Å, c = 187.65 Å. The asymmetric unit contains one monomer according to a solvent content of 68% (V_m = 3.79 $Å^3$ Da^{-1}). Under cryoconditions the cell constants changed to a = b = 105.48 Å, c = 187.70 Å.

Data collection and processing

Data sets to 2.7 Å were collected with a Mar Research imaging plate system with graphite monochromatized Cu-K_α radiation from a Rigaku RU200 rotation anode generator. Because of the low stability of the crystals in the X-ray beam, only 15 frames could be measured from one crystal at a temperature of 4°C. A complete data set to 2.9 Å resolution was obtained by merging data sets collected from five crystals. In order to reduce the crystal degradation during data collection, crystals were flash cooled in a 95K nitrogen beam in the presence of 25% glycerol as cryoprotectant. Under these conditions a complete data set to 2.7 Å resolution was collected from one crystal. Diffraction data to a resolution of 2.1 Å have been collected from a cryofrozen crystal at the BW6 beamline at DESY (Hamburg; λ = 1.1 Å).

All data were evaluated with MOSFLM [106], and scaled and merged with the CCP4 package [107]. A total number of 30,205 unique reflections (111,661 total measurements) was collected for the high-resolution data set. The data are 97.9% complete to a resolution of 2.1 Å with an R_{merge} on intensities of 8.9% (Table 7).

Patterson search methods

The crystal structure of TmLDH was solved by Patterson search techniques [108,109]. A homology model was used based on the crystal structures of BsLDH [43], BlLDH [45], and SaLDH [48] as search model [14]. The flexible surface loop (Gln210B–Lys222) was omitted in the model. The program AMoRe [110] was used for Patterson search calculations in the resolution range from 15.0 Å to 3.5 Å with an integration vector of 20 Å. A unique solution was found with a correlation coefficient of 0.34 and an R factor of 49% compared to the next highest peak with values of 0.27 and 52%. The correct solution was verified by building up the native tetramer applying crystallographic symmetry to the monomeric model.

Model building and refinement

Model building was performed using the program O [111]. Crystallographic refinement was carried out with the program X-PLOR [112] (Table 7). Sidechains of amino acid residues, which showed no or only weak electron density, were omitted from the refinement. Lacking the last seven C-terminal residues, because of low occupancy in the electron-density map, the final model comprises 312 of 319 amino acid residues and includes NAD, fructose-1,6-bisphosphate, oxamate, and three cadmium ions. 344 solvent molecules have been placed into a well defined F_o–F_c electron-density map contoured at 3σ and into a $2F_o$–F_c electron-density map contoured at 1σ. The crystallographic R factor of the final model is 20.0% for all unique reflections from 8.0–2.1 Å (R_{free} = 28.6%). The rms deviations from ideal stereochemistry are 0.010 Å for bond lengths and 1.91° for bond angles [113]. The averaged B factor for the protein model is 35.4 $Å^2$. The stereochemistry of the model was verified using the program PROCHECK [114]. The Ramachandran plot [115] reveals all dihedral angles of the polypeptide

Table 7

Data collection and refinement statistics.

Data collection	
Resolution range (Å)	20.0–2.1
Observed reflections	111,661
Unique reflections	30,205
R_{merge}*	0.089
Completeness (%) (overall/outer shell)	97.9/96.5
B factor from Wilson plot ($Å^2$)	28.3
Refinement	
Resolution range (Å)	20.0–2.1
R_{cryst}	0.200
R_{free}†	0.286
Number of protein atoms	2403
Number of water molecules	334
Rmsd‡ bond lengths (Å)	0.010
Rmsd‡ angles (°)	1.91
Mean B factor	
protein ($Å^2$)	35.4
solvent ($Å^2$)	63.7

*$R_{merge} = \Sigma|I_i - \langle I \rangle I / \Sigma I_i$, where I_i is the intensity of an individual reflection and $\langle I \rangle$ is the mean intensity of that reflection. †R_{free} is the cross-validation R_{factor} computed for the test set of reflections (5% of total) which were omitted in the refinement process. ‡Root mean square deviation from ideality.

backbone in allowed regions of the psi–phi diagram. Secondary structure elements of TmLDH are assigned according to the algorithm of DSSP [116]. The multiple sequence alignment was performed using the program PILEUP [117] and rendered graphically with ALSCRIPT [118]. Ribbon representations of the mainchain folding of the molecule were drawn using the programs MOLSCRIPT [119] and RENDER [120].

Structural comparison

The program HBPlus was used for locating hydrogen bonds [121]. Ion-pair analysis was performed using X-PLOR with distance cut-offs of 4 Å [79] or 6 Å, respectively. Residues Ala, Ile, Leu, Met, Phe, Pro, Trp, and Val were assigned as hydrophobic, residues Ser, Thr, Gln, Asn, Gly, Cys, and Tyr, as polar, and residues Asp, Glu, Lys, and Arg as charged. Surfaces, volumes, and cavities were calculated with the programs GRASP [122], VOIDOO [123], and X-PLOR. For cavity calculations all water and ligand molecules were truncated from the coordinates and a probe radius of 1.4 Å was used. As the resolution of LcLDH is 3.0 Å, the results derived from this structure have been treated with caution and excluded from some comparison tables. Despite the fact, that the structural deviations of the differently liganded crystal structures of SsLDH and SaLDH are rather small (Table 1), only the NADH–oxamate complex structures of each species were used for structural comparisons.

Accession numbers

The coordinates of TmLDH have been deposited in the Brookhaven Protein Data Bank, with accession code 1a5z.

Acknowledgements

The excellent technical assistance of Barbara Kellerer (Regensburg) is gratefully acknowledged. We thank Hans Bartunik and his group for expert support during measurements at the beamline BW6 at DESY (Hamburg) and Tarmo Ploom (Martinsried) for fruitful discussions.

References

1. Achenbach-Richter, L., Gupta, R., Stetter, K.O. & Woese, C.R. (1987). Were the original eubacteria thermophiles? *System. Appl. Microbiol.* **9**, 34-39.
2. Huber, R., Langworthy, T.A., König, H., Thomm, M., Woese, C.R., Sleytr, U.B. & Stetter, K.O. (1986). *Thermotoga maritima* sp. nov. represents a new genus of unique extremely thermophilic eubacteria growing up to 90°C. *Arch. Microbiol.* **144**, 324-333.
3. Dams, T., Böhm, G., Auerbach, G., Bader, G., Schurig, H. & Jaenicke, R. (1998). Homo-dimeric recombinant dihydrofolate reductase from *Thermotoga maritima* shows extreme intrinsic stability. *Biol. Chem.* **379**, 367-371.
4. Schurig, H., Rutkat, K., Rachel, R. & Jaenicke, R. (1995). Octameric enolase from the hyperthermophilic bacterium *Thermotoga maritima*: purification, characterization, and image processing. *Protein Sci.* **4**, 228-236.
5. Darimont, B. & Sterner, R. (1994). Sequence, assembly and evolution of a primordial ferredoxin from *Thermotoga maritima. EMBO J.* **13**, 1772-1781.
6. Kort, R., Liebl, W., Labedan, B., Forterre, B., Eggen, R.J.L. & Devos, W.M. (1997). Glutamate dehydrogenase from the hyperthermophilic bacterium *Thermotoga maritima* – molecular characterization and phylogenetic implications. *Extremophiles* **1**, 52-60.
7. Wrba, A., Schweiger, A., Schultes, V., Jaenicke, R. & Závodszky, P. (1990). Extremely thermostable D-glyceraldehyde-3-phosphate dehydrogenase from the eubacterium *Thermotoga maritima. Biochemistry* **29**, 7584-7592.
8. Schultes, V., Deutzmann, R. & Jaenicke, R. (1990). Complete amino-acid sequence of glyceraldehyde-3-phosphate dehydrogenase from the hyperthermophilic eubacterium *Thermotoga maritima. Eur. J. Biochem.* **192**, 25-31.
9. Tomschy, A., Glockshuber, R. & Jaenicke, R. (1993). Functional expression of D-glyceraldehyde-3-phosphate dehydrogenase from the hyperthermophilic eubacterium *Thermogota maritima* in *Escherichia coli:* authenticity and kinetic properties of the recombinant enzyme. *Eur. J. Biochem.* **214**, 43-50.
10. Tomschy, A., Böhm, G. & Jaenicke, R. (1994). The effect of ion pairs on the thermal stability of D-glyceraldehyde-3-phosphate dehydrogenase from the hyperthermophilic bacterium *Thermotoga maritima. Protein Eng.* **7**, 1471-1478.
11. Hecht, K., Wrba, A. & Jaenicke, R. (1989). Catalytic properties of thermophilic lactate dehydrogenase and halophilic malate dehydrogenase at high temperature and low water activity. *Eur. J. Biochem.* **183**, 69-74.
12. Wrba, A., Jaenicke, R., Huber, R. & Stetter, K.O. (1990). Lactate dehydrogenase from the extreme thermophile *Thermotoga maritima. Eur. J. Biochem.* **188**, 195-201.
13. Ostendorp, R., Liebl, W., Schurig, H. & Jaenicke, R. (1993). The L-lactate dehydrogenase gene from the hyperthermophilic bacterium *Thermotoga maritima* cloned by complementation in *Escherichia coli. Eur. J. Biochem.* **216**, 709-715.
14. Ostendorp, R., Auerbach, G. & Jaenicke, R. (1996). Extremely thermostable L(+)-lactate dehydrogenase from *Thermotoga maritima*: cloning, characterization, and crystallization of the recombinant enzyme in its tetrameric and octameric state. *Protein Sci.* **5**, 862-873.
15. Dams, T., Ostendorp, R., Ott, M., Rutkat, K. & Jaenicke, R. (1996). Tetrameric and octameric lactate dehydrogenase from the hyperthermophilic bacterium *Thermotoga maritima. Eur. J. Biochem.* **240**, 274-279.
16. Schurig, H., Beaucamp, N., Ostendorp, R., Jaenicke, R., Adler, E. & Knowles, J. (1995). PGK and TIM from the hyperthermophilic bacterium *Thermotoga maritima* form a covalent bifunctional enzyme complex. *EMBO J.* **14**, 442-451.
17. Grättinger, M., Dankesreiter, A., Schurig, H. & Jaenicke, R. (1998). Recombinant PGK from the hyperthermophilic bacterium *Thermotoga maritima*: catalytic, spectral and thermodynamic properties. *J. Mol. Biol.*, in press.
18. Sterner, R., Kleemann, J.R., Szadkowski, H., Hennig, M. & Kirschner, K. (1996). Phosphoribosyl anthranilate isomerase from *Thermotoga maritima* is an extremely stable and active homodimer. *Protein Sci.* **5**, 2000-2008.
19. Wassenberg, D., Schurig, H., Liebl, W. & Jaenicke, R. (1997). Xylanase XynA from the hyperthermophilic bacterium *Thermotoga maritima*: structure and stability of the recombinant enzyme and its isolated cellulose-binding domain. *Protein Science* **6**, 1718-1726.
20. Macedo-Ribeiro, S., Darimont, B., Sterner, R. & Huber, R. (1996). Small structural changes account for the high thermostability of 1[4Fe–4S] ferredoxin from the hyperthermophilic bacterium *Thermotoga maritima. Structure* **4**, 1291-1301.
21. Korndörfer, I., Steipe, B., Huber, R., Tomschy, A. & Jaenicke R. (1995). The crystal structure of holo-glyceraldehyde-3-phosphate dehydrogenase from the hyperthermophilic bacterium *Thermotoga maritima* at 2.5 Å resolution. *J. Mol. Biol.* **246**, 511-521.
22. Knapp, S., de Vos, W.M., Rice, D. & Ladenstein, R. (1997). Crystal structure of glutamate dehydrogenase from the hyperthermophilic eubacterium *Thermotoga maritima* at 3.0 Å resolution. *J. Mol. Biol.* **267**, 916-932.
23. Auerbach, G., *et al.*, & Jacob, U. (1997). Closed structure of phosphoglycerate kinase from *Thermotoga maritima* reveals the catalytic mechanism and determinants of thermal stability. *Structure* **5**, 1475-1483.
24. Auerbach, G., Jacob, U., Grättinger, M., Schurig, H. & Jaenicke, R. (1997). Crystallographic analysis of phosphoglycerate kinase from the hyperthermophilic bacterium *Thermotoga maritima. Biol. Chem.* **378**, 327-329.
25. Hennig, M., Sterner, R., Kirschner, K. & Jansonius, J.N. (1997). Crystal structure at 2.0 Å resolution of phoshoribosyl anthranilate isomerase from the hyperthermophile *Thermotoga maritima*: possible determinants of protein stability. *Biochemistry* **36**, 6009-6016.
26. Rossmann, M.G., Liljas, A., Brändén, C.-I. & Banaszak, L.J. (1975). Evolutionary and structural relationships among dehydrogenases. In *The Enzymes.* (Boyer, P.D., ed.), third edition, 11, pp. 61-102, Academic Press, New York.
27. Jaenicke, R. (1987). Folding and association of proteins. *Prog. Biophys. Mol. Biol.* **49**, 117-237.
28. Holbrook, J.J., Liljas, A., Steindel, S.J. & Rossmann, M.G. (1975). Lactate dehydrogenase. In *The Enzymes.* (Boyer, P.D., ed.), third edition, **11**, pp. 191-292, Academic Press, New York.
29. Clarke, A.R., Atkinson, T. & Holbrook, J.J. (1980). From analysis to synthesis: new ligand binding sites on the lactate dehydrogenase framework. *Trends Biochem. Sci.* **14**, 101-105.
30. Jaenicke, R. (1991). Protein stability and molecular adaptation to extreme conditions. *Eur. J. Biochem.* **202**, 715-728.
31. Argos, P., Rossmann, M.G., Grau, U.M., Zuber, H., Frank, G. & Tratschin, J.D. (1979). Thermal stability and protein structure. *Biochemistry* **18**, 5698-5703.

32. Menéndez-Arias, L. & Argos, P. (1989). Engineering protein thermal stability. Sequence statistics point to residue substitutions in α-helices. *J. Mol. Biol.* **206**, 397-406.
33. Zuber, H. (1978). Comparative studies of thermophilic and mesophilic enzymes: objectives, problems, results. In *Biochemistry of Thermophily.* (Friedman, S.M., ed.), pp. 267-285, Academic Press, New York.
34. Zuber, H. (1988). Temperature adaptation of lactate dehydrogenase. Structural, functional and genetic aspects. *Biophys. Chem.* **29**, 171-179.
35. Zülli, F., Weber, H. &, Zuber, H. (1990). Analysis of structural elements responsible for the differences in thermostability and activation by fructose 1,6-bisphosphate in lactate dehydrogenase from *B. stearothermophilus* and *B. caldolyticus* by protein engineering. *Biol. Chem.* **371**, 655-662.
36. Zülli, F., Schneiter, R., Urfer, R. & Zuber, H. (1991). Engineering thermostability and activity of lactate dehydrogenase from Bacilli. *Biol. Chem.* **372**, 363-372.
37. Vogt, G., Woell, S. & Argos, P. (1997). Protein thermal stability, hydrogen bonds, and ion pairs. *J. Mol. Biol.* **269**, 631-643.
38. Böhm, G. & Jaenicke, R. (1994). Relevance of sequence statistics for the properties of extremophilic proteins. *Int. J. Peptide Protein Res.* **43**, 97-106.
39. Jaenicke, R. (1996). Stability and folding of ultrastable proteins: eye lens crystallins and enzymes from thermophiles. *FASEB J.* **10**, 84-92.
40. Vieille, C. & Zeikus, J.G. (1996). Thermozymes: identifying molecular determinants of protein structural and functional stability. *Trends Biotech.* **14**, 183-190.
41. Colacino, F. & Crichton, R.R. (1997). Enzyme thermostabilization: the state of the art. *Biotech. Genet. Eng. Rev.* **14**, 211-277.
42. Piontek, K., Chakrabarti, P., Schär, H.-P., Rossmann, M.G. & Zuber, H. (1990). Structure determination and refinement of *Bacillus stearothermophilus* lactate dehydrogenase. *Proteins* **7**, 74-92.
43. Wigley, D.B., *et al.*, & Holbrook, J.J. (1992). Structure of a ternary complex of an allosteric lactate dehydrogenase from *Bacillus stearothermophilus* at 2.5 Å resolution. *J. Mol. Biol.* **223**, 317-335.
44. Buehner, M., Ford, G.C., Olsen, K.W., Moras, D. & Rossmann, M.G. (1974). Three-dimensional structure of D-glyceraldehyde-3-phosphate dehydrogenase. *J. Mol. Biol.* **82**, 563-585.
45. Iwata, S., Kamata, K., Yoshida, S., Minowa, T. & Ohta, T. (1994). T and R states in the crystals of bacterial L-lactate dehydrogenase reveal the mechanism for allosteric control. *Nat. Struct. Biol.* **1**, 176-185.
46. Adams, M.J., *et al.*, & Wonacott, A.J. (1970). Structure of lactate dehydrogenase at 2.8 Å resolution. *Nature* **227**, 1098-1103.
47. White, R.H., *et al.*, & Rossmann, M.G. (1976). *J. Mol. Biol.* **102**, 759-779.
48. Abad-Zapatero, C., Griffith, J.P., Sussman, J.L. & Rossmann, M.G. (1987). Refined crystal structure of dogfish M_4 apo-lactate dehydrogenase. *J. Mol. Biol.* **198**, 445-467.
49. Hogrefe, H.H., Griffith, J.P., Rossmann, M.G. & Goldberg, E. (1987). Characterization of the antigenic sites on the refined 3-Å resolution crystal structure of mouse testicular lactate dehydrogenase. *J. Biol. Chem.* **262**, 13155-13162.
50. Grau, U.M., Trommer, W.E. & Rossmann, M.G. (1981). Structure of the active ternary complex of pig heart lactate dehydrogenase with S-lac-NAD at 2.7 Å resolution. *J. Mol. Biol.* **151**, 289-307.
51. Dunn, C.R., *et al.*, & Holbrook, J.J. (1996). The structure of lactate dehydrogenase form *Plasmodium falciparum* reveals a new target for anti-malarial design. *Nat. Struct. Biol.* **3**, 912-915.
52. Jaenicke, R., Schurig, H., Beaucamp, N. & Ostendorp, R. (1996). Structure and stability of hyperstable proteins: glycolytic enzymes from the hyperthermophilic bacterium *Thermotoga maritima*. *Adv. Protein Chem.* **48**, 181-269.
53. Kellis, J.T., Jr., Nyberg, K., Sali, D.D. & Fersht, A. (1988). Contribution of hydrophobic interactions to protein stability. *Nature* **333**, 784-786.
54. Privalov, P.L. (1988). Stability of protein structure and hydrophobic interaction. *Adv. Prot. Chem.* **39**, 191-234.
55. Perutz, M.F. & Raidt, H. (1975). Stereochemical basis of heat stability in bacterial ferredoxins and in haemoglobin A2. *Nature* **255**, 256-259.
56. Spassov, V.Z., Karshikoff, A.D. & Ladenstein, R. (1994). Optimization of the electrostatic interactions in proteins of different functional and folding type. *Protein Sci.* **3**, 1556-1569.
57. Baker, E.N. & Hubbard, R.E. (1984). Hydrogen bonding in globular proteins. *Prog. Biophys. Mol. Biol.* **44**, 97-179.
58. Vogt, G. & Argos, P. (1997). Protein thermal stability: hydrogen bonds or internal packing. *Fold. Des.* **2**, S40-S46.
59. Chothia, C.H. (1976). The nature of the accessible and buried surfaces in proteins. *J. Mol. Biol.* **105**, 1-14.
60. Wodak, S., Crombrugghe, D. & Janin, J. (1987). Computer studies of interaction between macromolecules. *Prog. Biophys. Mol. Biol.* **49**, 29-43.
61. Eriksson, A.E., *et al.*, & Matthews, B.W. (1992). Response of a protein structure to cavity-creating mutations and its relation to the hydrophobic effect. *Science* **255**, 178-183.
62. Marqusee, S. & Baldwin, R.L. (1987). Helix stabilization by Glu–Lys+ salt bridges in short peptides of *de novo* design. *Proc. Natl Acad. Sci. USA* **84**, 8898-8902.
63. Sundaralingam, S., Sekharudu, Y.C., Yathindra, N. & Ravichandran, V. (1987). Ion pairs in alpha helices. *Proteins* **2**, 64-71.
64. Nicholson, H., Becktel, W.J. & Matthews, B.W. (1988). Enhanced thermostability from designed mutations that interact with α-helix dipoles. *Nature* **336**, 651-656.
65. Sali, D., Bycroft, M. & Fersht, A.R. (1988). Stabilization of protein structure by interaction of α-helix dipole with a charged sidechain. *Nature* **335**, 496-500.
66. Serrano, L. & Fersht, A.R. (1989). Capping and α-helix stability. *Nature* **342**, 296-299.
67. Hart, K.W., *et al.*, & Holbrook, J.J. (1987). A strong carboxylate-arginine interaction is important in substrate orientation and recognition in lactate dehydrogenase. *Biochim. Biophys. Acta* **914**, 294-298.
68. Ostendorp, R. (1996). *Untersuchungen zur Struktur, Stabilität und Faltung extrem thermophiler Proteine: Die Laktat Dehydrogenase aus* Thermotoga maritima *in ihrer tetrameren und oktameren Erscheinungsform.* PhD thesis, University of Regensburg, Germany.
69. Than, M.E., *et al.*, & Soulimane, T. (1997). *Thermus thermophilus* cytochrome-c552: a new highly thermostable cytochrome-c structure obtained by MAD phasing. *J. Mol. Biol.* **271**, 629-644.
70. Auerbach, G. (1997). *Röntgenstrukturanalyse der Enzyme des Tetrahydrobiopterin-Biosynthesewegs und hyperthermophiler Enzyme aus* Thermotoga maritima. PhD thesis. Technical University of Munich, Germany.
71. Kauzmann, W. (1959). Some factors in the interpretation of protein denaturation. *Adv. Protein Chem.* **14**, 1-63.
72. Matthews, B.W. (1995). Studies on protein stability with T4 lysozyme. *Adv. Protein Chem.* **46**, 249-278.
73. Wierenga, R.K., Noble, M.E.M. & Davenport, R.C. (1992). Comparison of the refined crystal structures of liganded and unliganded chicken, yeast and trypanosomal triosephosphate isomerase. *J. Mol. Biol.* **224**, 1115-1126.
74. Hubbard, S.J., Gross, K.-H. & Argos, P. (1994). Intramolecular cavities in globular proteins. *Protein Eng.* **7**, 613-626.
75. Chan, M.K., Mukund, S., Kletzin, A., Adams, M.W.W. & Rees, D.C. (1995). Structure of a hyperthermophilic tungstopterin enzyme, aldehyde ferredoxin oxidoreductase. *Science* **267**, 1463-1469.
76. Lee, B. & Richards, F.M. (1971). The interpretation of protein structure: estimation of static accessibility. *J. Mol. Biol.* **55**, 379-400.
77. Connolly, M.L. (1983). Solvent-accessible surface of proteins and nucleic acids. *Science* **221**, 709-713.
78. Hilbert, M., Böhm, G. & Jaenicke, R. (1993). Structural relationships of homologous proteins as a fundamental principle in homology modeling. *Proteins* **17**, 138-151.
79. Barlow, D.J. & Thornton, J.M. (1983). Ion-pairs in proteins. *J. Mol. Biol.* **168**, 867-885.
80. Mrabet, N.T., *et al.*, & Wodak, S.J. (1992). Arginine residues as stabilizing elements in proteins. *Biochemistry* **31**, 2239-2253.
81. Borders, C.L., Jr., *et al.*, & Pett, V. (1994). A structural role for arginine in proteins: multiple hydrogen bonds to backbone carbonyl oxygens. *Protein Sci.* **3**, 541-548.
82. Suzuki, Y., Hatagaki, K. & Oda, H. (1991). A hyperthermostable pullulanase produced by an extreme thermophile, *Bacillus flavocaldarius* KP 1228, and evidence for the proline theory of increasing protein thermostability. *Appl. Microbiol. Biotechnol.* **34**, 707-714.
83. Van den Burg, B., Vriend, G., Veltman, O.R., Venema, G. & Eijsink, V.G.H. (1998). Engineering an enzyme to resist boiling. *Proc. Natl Acad. Sci.* **95**, 2056-2060.
84. Sharp, K.A. & Honig, B. (1990). Electrostatic interactions in macromolecules: theory and applications. *Annu. Rev. Biophys. Chem.* **19**, 301-332.
85. Stigter, D. & Dill, K.A. (1990). Charge effects on folded and unfolded proteins. *Biochemistry* **29**, 1262-1271.
86. Anderson, D.E., Becktel, W.J. & Dahlquist, F.W. (1990). pH-induced denaturation of proteins – a single salt-bridge contributes 3–5 kcal/mol to the free energy of folding of T4-lysozyme. *Biochemistry* **29**, 2403-2408.

87. Honig, B. & Nicolls, A. (1995). Classical electrostatics in biology and chemistry. *Science* **268**, 1144-1149.
88. Russell, R.J.M., Hough, D.W., Danson, M.J. & Taylor, G.L. (1994). The crystal structure of citrate synthase from the thermophilic Archaeon, *Thermoplasma acidophilum*. *Structure* **2**, 1157-1167.
89. Hennig, M., Darimont, B., Sterner, R., Kirschner, K. & Jansonius, J.N. (1995). 2.0 Å structure of indole-3-glycerol phosphate synthase from the hyperthermophile *Sulfolobus solfataricus*: possible determinants of protein stability. *Structure* **3**, 1295-1306.
90. Kelly, C.A., Nishiyama, M., Ohnishi, Y., Beppu, T. & Birktoft, J.J. (1993). Determination of protein stability in the 1.9 Å crystal structure of malate dehydrogenase from the thermophilic bacterium *Thermus flavus*. *Biochemistry* **32**, 3913-3922.
91. Yip, K.S.P., *et al*., & Rice, D.W. (1995). The structure of *Pyrococcus furiosus* glutamate dehydrogenase reveals a key role for ion-pair networks in maintaining enzyme stability at extreme temperatures. *Structure* **3**, 1147-1158.
92. Horovitz, A., Serrano, L., Avron, B., Bycroft, M. & Fersht, A.R. (1990). Strength and cooperativity of contributions of surface salt bridges to protein stability. *J. Mol. Biol.* **216**, 1031-1044.
93. Pappenberger, G., Schurig, H. & Jaenicke, R. (1997). Disruption of an ionic network leads to accelerated thermal denaturation of D-glyceraldehyde-3-phosphate dehydrogenase from the hyperthermophilic bacterium *Thermotoga maritima*. *J. Mol. Biol.* **274**, 676-683.
94. Hol, W.G. (1985). The role of the α-helix dipole in protein function and structure. *Prog. Biophys. Mol. Biol.* **45**, 149-195.
95. Matthews, B.W. (1993). Structural and genetic analysis of protein stability. *Annu. Rev. Biochem.* **62**, 139-160.
96. Fersht, A.R. & Serrano, L. (1993). Principles of protein stability derived from protein engineering experiments. *Curr. Opin. Struct. Biol.* **3**, 75-83.
97. Careri, G., Gratton, E., Yang, P.-H. & Rupley, J.A. (1980). Correlation of IR spectroscopic, heat capacity, diamagnetic susceptibility and enzymatic measurements on lysozyme powder. *Nature* **284**, 572-573.
98. Richards, F.M. (1974). The interpretation of protein structure: total volume, group volume, distributions and packing density. *J. Mol. Biol.* **82**, 1-14.
99. Chothia, C.H. (1974). Hydrophobic bonding and accessible surface area in proteins. *Nature* **248**, 338-339.
100. Pakula, A.A. & Sauer, R.T. (1989). Genetic analysis of proteins stability and function. *Annu. Rev. Genet.* **23**, 289-310.
101. Alber, T., Dao-Pin, S., Nye, J.A., Muchmore, D.C. & Matthews, B.W. (1987). Temperature-sensitive mutants of bacteriophage T4 lysozyme occur at sites with low mobility and low solvent accessibility in the folded protein. *Biochemistry* **26**, 3754-3758.
102. Matsumara, M., Becktel, W.J. & Matthews, B.W. (1988). Hydrophobic stabilization in T4 lysozyme determined directly by multiple substitutions of Ile3. *Nature* **334**, 406-410.
103. Kohlhoff, H., Dahm, A. & Hensel, R. (1996). Tetrameric triosephosphate isomerase from hyperthermophilic archaea. *FEBS Lett.* **383**, 245-250.
104. Beaucamp, N., Hofmann, A., Kellerer, B. & Jaenicke, R. (1997). Dissection of the gene of the bifunctional PGK–TIM fusion protein from the hyperthermophilic bacterium *Thermotoga maritima*: design and characterization of the separate triosephosphate isomerase. *Protein Sci.* **6**, 2159-2165.
105. Beaucamp, N., Ostendorp R., Schurig, H. & Jaenicke, R. (1995). Cloning, sequencing, expression and characterization of the gene encoding the 3-phosphoglycerate kinase triosephosphate isomerase fusion protein from *Thermotoga maritima*. *Protein Pept. Lett.* **2**, 287-290.
106. Leslie, A.G.W. (1991). Macromolecular data processing. In *Crystallographic Computing*. (Moras, V.D., Podjarny, A.D. & Thierry, J.C. eds), pp. 27-38, Oxford University Press, Oxford, UK.
107. Collaborative Computational Project, Number 4 (1994). The CCP4 suite: programs for protein crystallography. *Acta Cryst. D* **50**, 760-763.
108. Huber, R. (1965). Die automatisierte Faltmolekülmethode. *Acta Cryst. A* **15**, 23-31.
109. Rossmann, M.G. (1990). The molecular replacement method. *Acta Cryst. A* **46**, 73-82.
110. Navaza, J. & Vernoslava, E. (1994). On the fast-translation functions for molecular replacement. *Acta Cryst. A* **51**, 445-449.
111. Jones, T.A., Beydoll, M. & Kjeldgaard, M. (1990). O: a macromolecule modelling environment. In *Crystallography and Modelling Methods in Molecular Design*. (Bugg, C. & Ealick, S., eds), pp. 189-199, Springer-Verlag, New York.
112. Brünger, A.T. (1992). X-PLOR: a system for crystallography and NMR. Yale University Press, New Haven, CT.
113. Engh, R.A. & Huber R. (1991). Accurate bond and angle parameters for X-ray protein structure and refinement. *Acta Cryst. A* **47**, 392-400.
114. Laskowski, R.A., MacArthur, M.W., Moss, D.S. & Thornton, J.M. (1993). PROCHECK: a program to check the stereochemical quality of protein structures. *J. Appl. Cryst.* **26**, 283-291.
115. Ramachandran, G.N. & Sasisekharan, V. (1968). Conformation of polypeptides and proteins. *Adv. Protein Chem.* **23**, 283-437.
116. Kabsch, W. & Sander, C. (1983). Dictionary of protein secondary structure: pattern recognition of hydrogen bonded and geometrical features. *Biopolymers* **22**, 2577-2637.
117. Genetics Computer Group (GCG) (1997). Wisconsin Package Version 9.1. Madison, Wisconsin.
118. Barton, G.J. (1993). ALSCRIPT: a tool to format multiple sequence alignments. *Protein Eng.* **6**, 37-40.
119. Kraulis, P.J. (1991). MOLSCRIPT: a program to produce both detailed and schematic plots of protein structures. *J. Appl. Cryst.* **24**, 946-950.
120. Merritt, E.A. & Murphy, M.E.P. (1994). Raster3D version 2.0: a program for photorealistic molecular graphics. *Acta Cryst. D* **50**, 869-873.
121. McDonald, I. & Thornton, J. (1994). Satisfying hydrogen bonding potential in proteins. *J. Mol. Biol.* **238**, 777-793.
122. Nicholls, A., Bharadwaj, R. & Honig, B. (1993). Grasp – graphical representation and analysis of surface properties. *Biophys. J.* **64**, A166.
123. Kleywegt, G.J. & Jones, A.T. (1994). Detection, delineation, measurement and display of cavities in macromolecular structures. *Acta Cryst. D* **50**, 178-185.
124. Eventoff, W., *et al*., & Kiltz, H.-H. (1977). Structural adaptations of lactate dehydrogenase isozymes. *Proc. Natl Acad. Sci. USA* **74**, 2677-2681.